LSD1-mediated repression of GFI1 super-enhancer plays an essential role in erythroleukemia.

LSD1-mediated repression of *GFI1* super-enhancer plays an essential role in erythroleukemia

Goichi Tatsumi[1,2], Masahiro Kawahara[2]*, Ryusuke Yamamoto[1], Masakatsu Hishizawa[1], Katsuyuki Kito[2], Takayoshi Suzuki[3,4], Akifumi Takaori-Kondo[1] and Akira Andoh[2]

Affiliations

[1] Department of Hematology and Oncology, Graduate School of Medicine, Kyoto University.

[2] Department of Medicine, Shiga University of Medical Science.

[3] The Institute of Scientific and Industrial Research, Osaka University.

[4] CREST, Japan Science and Technology Agency (JST)

Contact information

*Corresponding author: Masahiro Kawahara

E-mail: mkawahar@belle.shiga-med.ac.jp

Address: Seta-Tsukinowa, Otsu, Shiga, 520-2192, Japan

Tel: +81-77-548-2217

Fax: +81-77-548-2219

Running title: *GFI1* super-enhancer repression by LSD1 in leukemia

Supplementary Information

includes

Supplementary Materials and Methods

Supplementary Figures 1-13

Supplementary Tables 1-3

Supplementary materials and methods

Cells

THP-1 cells and murine erythroleukemia cells (MEL) were cultured in RPMI 1640 medium supplemented with 10% fetal bovine serum (FBS) and 1% penicillin. MDS-L cells[1] were cultured in the same medium with 20 ng/ml human interleukin-3 (PeproTech, Rocky Hill, NJ) and 20 μM 2-mercaptoethanol.

Quantitative PCR

RNA was extracted using either TRIzol reagent (Life Technologies, Carlsbad, CA). Complementary RNA was synthesized by Superscript 3 reverse transcriptase (Thermo Fisher Scientific, Waltham, MA). Quantitative PCR was performed using LightCycler480 System II (Roche, Basel, Switzerland) and a THUNDERBIRD SYBR qPCR mix (Toyobo, Osaka, Japan). Absolute numbers were calculated using the recombinant DNA of targeted amplicons for the standard curve. The primer sequences are provided in Supplementary Table 1.

Western blotting

Total cell lysates were extracted in lysis buffer [50 mM Tris-HCl at pH 8.0, 150 mM NaCl,

1% Triton X, 1 mM PMSF, 1 mM EDTA, and protease inhibitor cocktail (Nacalai Tesque, Kyoto, Japan)]. We used primary antibodies anti-LSD1 (C69G12, Cell Signaling Technology, Tokyo, Japan) and anti-ACTIN (sc-1616, Santa Cruz Biotechnology, Dallas, TX). HRP-conjugated anti-rabbit (NA934v, GE Healthcare, Little Chalfont, UK) or anti-goat (sc-2020, Santa Cruz Biotechnology) were used as secondary antibodies.

Cell surface marker assay

For cell surface marker analysis, murine erythroleukemia cells were stained with anti-Ly6G(Gr-1)-PE-Cy7 (1A8; BD Biosciences, San Jose, CA), and human leukemia cells were stained with anti-CD11b-PE-Cy5 (ICRF44; eBioscience, San Diego, CA) and anti-CD235a-PE-Cy5 (GA-R2; BD Biosciences), and then analyzed by FACS Calibur or CantoII (BD Biosciences).

Cytology

Twenty-thousand cells were suspended in phosphate-buffered saline and attached to glass slides by centrifugation at 800 rpm for 4 minutes using Cytospin 4 (Thermo Fisher Scientific). The glass slides were stained with a traditional Wright-Giemsa staining.

Bisulfite sequencing

DNA methylation analysis was performed as described previously[2]. Briefly, genomic DNA was isolated from cells using QIAamp DNA Mini Kit (Qiagen, Hilden, Germany), and bisulfite treatment was performed using the MethylEasy Xceed Kit (Human Genetic Signatures, Sydney, Australia). Modified DNA was amplified by PCR and cloned into a pGEM-T Easy Vector System (Promega, Madison, WI). The bisulfite sequencing-specific primers are listed in Supplementary Table 1. The independent colonies were amplified with the Illustra TempliPhi Amplification kit (GE Healthcare) or NucleoSpin Plasmid EasyPure kit (Macherey-Nagel, Düren, Germany), and then sequenced.

Chromatin immunoprecipitation (ChIP)

ChIP was performed as described previously[3]. Briefly, after crosslinking with 0.5% paraformaldehyde for 10 min and quenching with 100 mM glycine for 10 min, cells were lysed and incubated in lysis buffer (50 mM HEPES pH 7.9, 140 mM NaCl, 1mM EDTA pH 8.0, 10% glycerol, 0.5% NP-40, 0.25% TritonX-10) on ice for 10 min. After intensive washes, the pellets were resuspended in shearing buffer (0.1% SDS, 1 mM EDTA pH 8.0, 10 mM

Tris-HCl pH 8.0) and sonicated using S220 ultrasonicators (Covaris, Woburn, MA). For precipitation, anti-H3K27ac (39133; Active Motif, Carlsbad, CA), anti-GFI1 (sc-376949; Santa Cruz Biotechnology), anti-GFI1B (sc-28356X; Santa Cruz Biotechnology), anti-CEBPA (sc-61X; Santa Cruz Biotechnology), anti-TAL1 (ab155195; Abcam, Cambridge, UK), anti-GATA1 (ab11852; Abcam), anti-RUNX1 (ab23980; Abcam), anti- ERG (ab133264; Abcam), anti-LSD1 (ab17721; Abcam), anti-CoREST (ab32631; Abcam), anti-HDAC1 (ab7028; Abcam) or anti-HDAC2 (ab7029; Abcam), and Dynabeads Protein G (Thermo Fisher Scientific) were used. After reverse crosslinking, ChIP DNA was purified with a MinElute PCR Purification kit (Qiagen) and analyzed by quantitative PCR.

Supplementary Figure 1

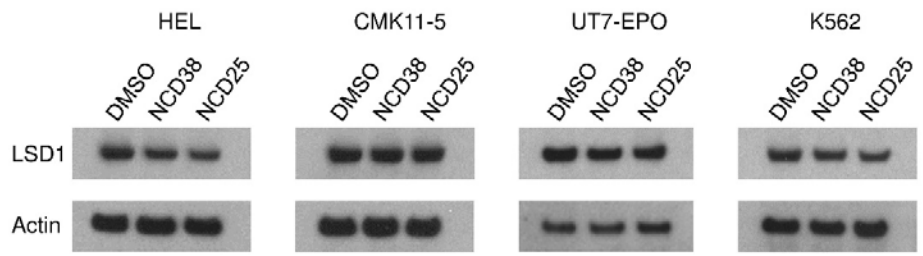

Supplementary Figure 1

LSD1 expression levels in erythro-megakaryocytic leukemia cell lines after exposure to NCD38 or NCD25

Western blot analysis for the protein expression level of LSD1 after 48-hour treatment with 2 μM NCD38, 2 μM NCD25, or DMSO. Actin was used as a control. Experiments were performed independently twice and representative data are shown.

Supplementary Figure 2

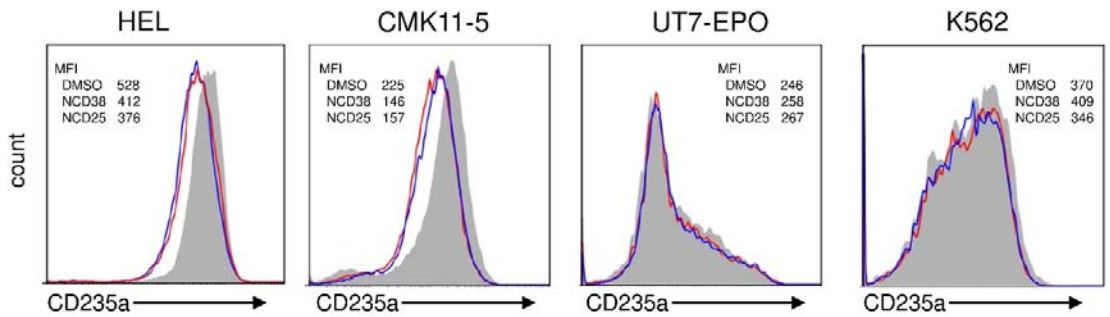

Supplementary Figure 2

Expression change of an erythroid marker, CD235a, in erythro-megakaryocytic leukemia cell lines after exposure to NCD38 or NCD25

FACS analysis of CD235a in HEL, CMK11-5, UT7-EPO and K562 cells after 48-hour treatment with 2 μM NCD38, 2 μM NCD25, or DMSO. The mean fluorescence intensity (MFI) is presented. Experiments were performed independently three times and representative data are shown.

Supplementary Figure 3

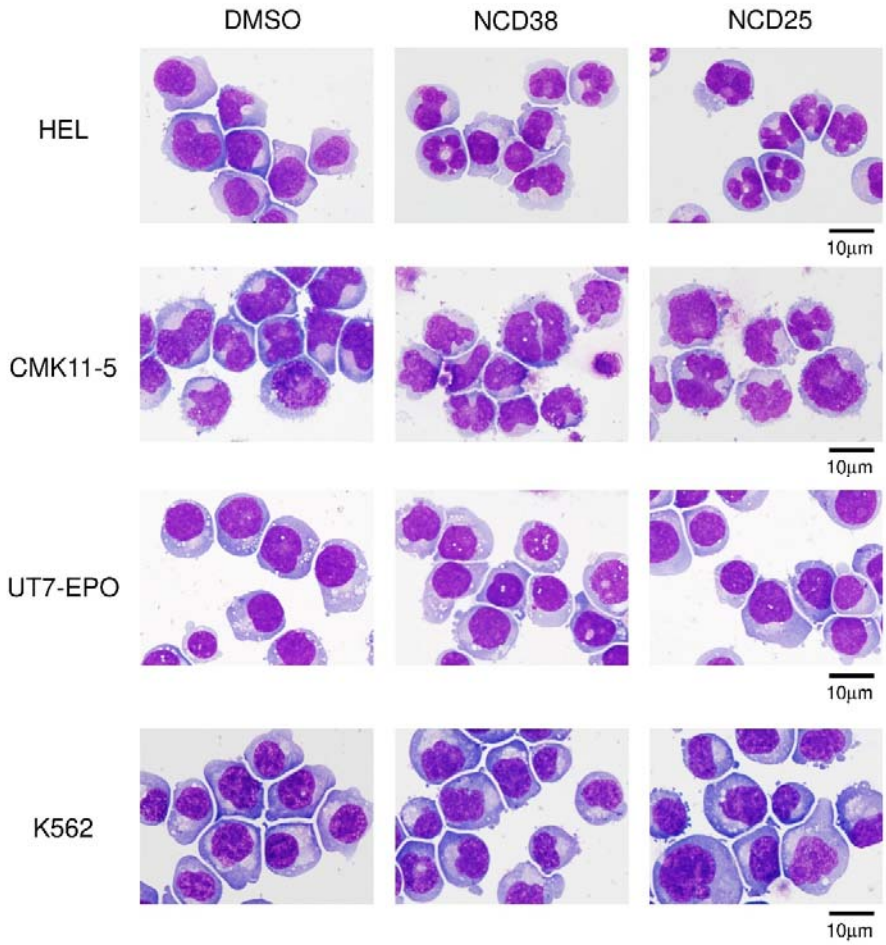

Supplementary Figure 3

Cytological changes in erythro-megakaryocytic leukemia cell lines after exposure to NCD38 or NCD25

Morphology of HEL, CMK11-5, UT7-EPO and K562 cells after 48-hour treatment with 2 μM NCD38, NCD25 or DMSO. Cytospin slides were stained with traditional Wright-Giemsa staining. Representative pictures are shown. Scale bar indicates 10 μm.

Supplementary Figure 4

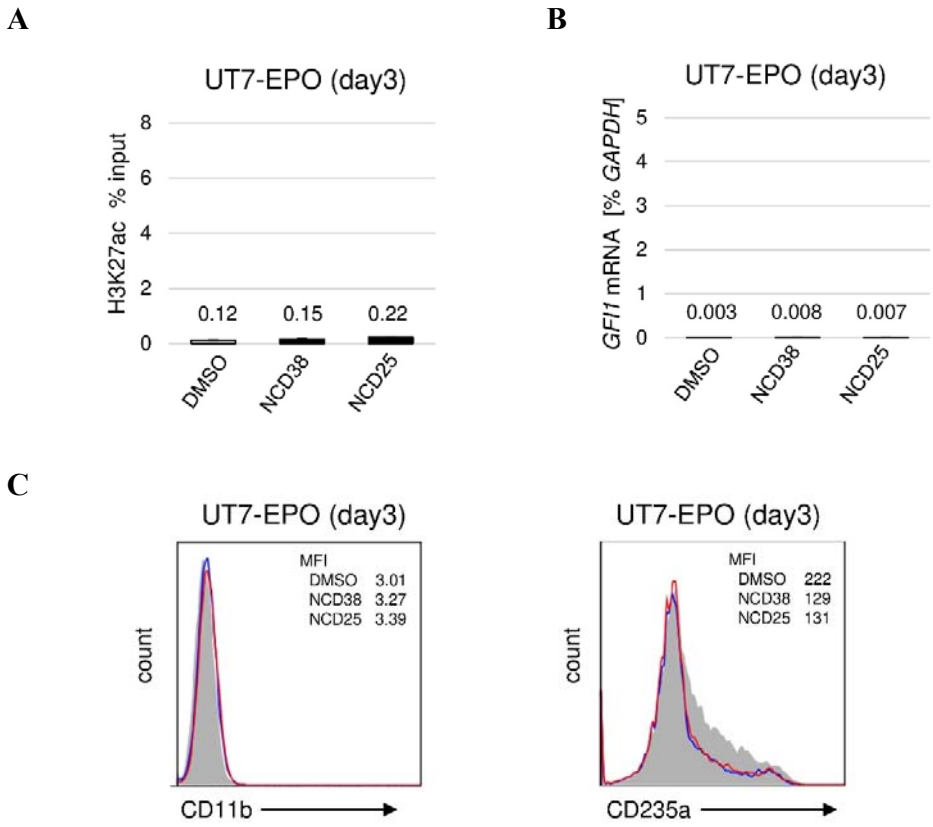

Supplementary Figure 4

H3K27ac in *GFI1*-SE, GFI1 transcript, and cell surface markers CD11b and CD235a in UT7-EPO cells after 72-hour treatment with NCD25 or NCD38

(a) ChIP-qPCR analysis of H3K27ac in *GFI1*-SE, (b) quantitative PCR analysis of the *GFI1* mRNA level and (c) FACS analysis of CD11b and CD235a in UT7-EPO cells after 72-hour treatment with 2 μM NCD38, 2 μM NCD25, or DMSO. The Y-axes in (a) and (b) indicate

the % input of H3K27ac and the % GAPDH, respectively. The mean fluorescence intensity (MFI) is presented in (c). All experiments were performed independently three times. The means (±SD) are shown in (a) and (b), and representative data are shown in (c).

Supplementary Figure 5

A

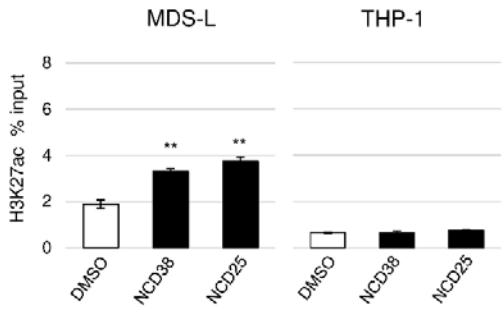

B

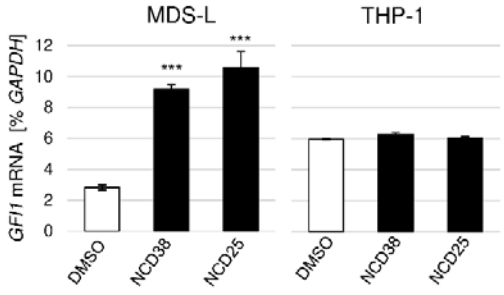

Supplementary Figure 5

***GFI1*-SE activation and *GFI1* expression status in MDS-L and THP-1 cells after exposure to NCD38 or NCD25**

(a) ChIP-qPCR analysis of H3K27ac in *GFI1*-SE and (b) quantitative PCR analysis of the *GFI1* mRNA level in MDS-L and THP-1 cells after 48-hour treatment with 2 μM NCD38, 2 μM NCD25, or DMSO. The Y-axes in (a) and (b) indicate the % input of H3K27ac and the % GAPDH. All experiments were performed independently three times and the means (±SD) are shown. *$p < 0.05$, **$p < 0.01$ and ***$p < 0.001$.

Supplementary Figure 6

A.

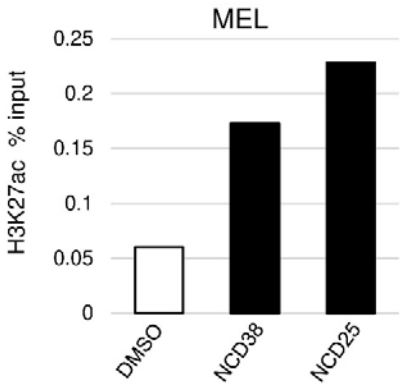

B.

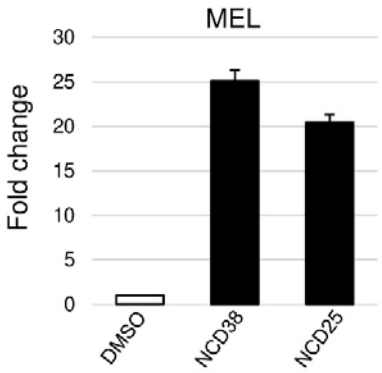

C.

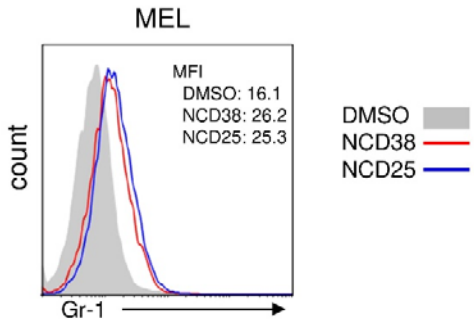

Supplementary Figure 6

Correlation of CA re-activation with myeloid differentiation in murine erythroleukemia

(MEL) cells

(a) ChIP-qPCR analysis of H3K27ac in the CA portion, (b) quantitative PCR analysis of the *Gfi1* mRNA level and (c) FACS analysis of Gr-1 in MEL cells after 48-hour treatment with LSD1 inhibitors including 2 μM NCD38 and 2 μM NCD25, or DMSO as a control. The Y-axes in (a) and (b) indicate % input of H3K27ac and the relative ratio of *Gfi1* mRNA in NCD38 or NCD25 to that in DMSO after normalization by the internal control *Gapdh* mRNA. Mean fluorescence intensity (MFI) is presented in (c). ChIP-qPCR and FACS experiments were performed independently twice. Quantitative PCR experiments were performed independently three times. The means (± SD) are shown in (a) and (b), and representative data are shown in (c).

Supplementary Figure 7

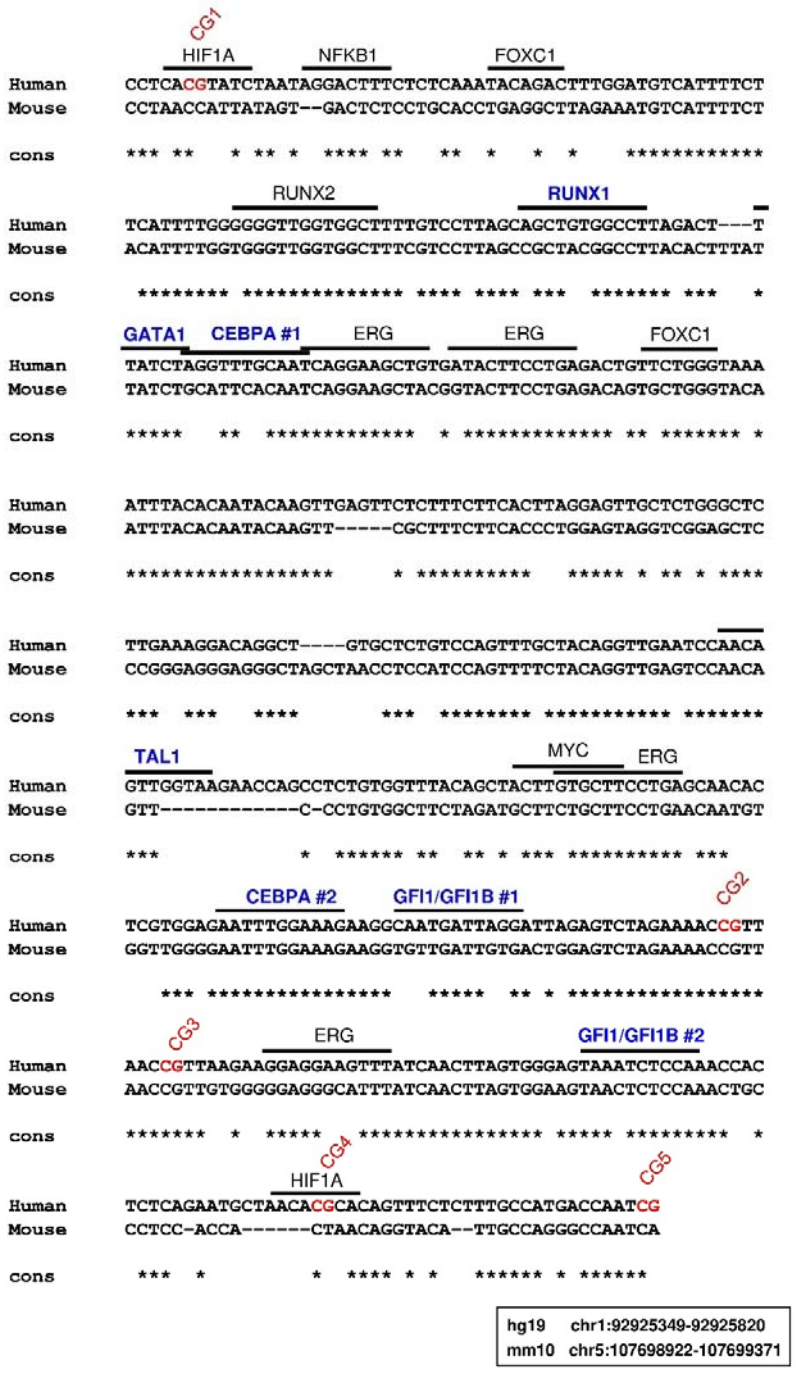

Supplementary Figure 7

TF motifs and CpG sites in the CA of *GFI1*-SE

Nucleotide sequence alignment between human and mouse of the CA of *GFI1*-SE. The lines above the sequences indicate the TF binding motifs that are related to myeloid differentiation. Several TF binding motifs presented in blue letters are the targets of mutagenesis in the luciferase assay (Fig. 2b). Five CpG sites in the CA of *GFI1*-SE are highlighted in red and each CpG site is numbered. The asterisks indicate the conserved nucleotides.

Supplementary Figure 8

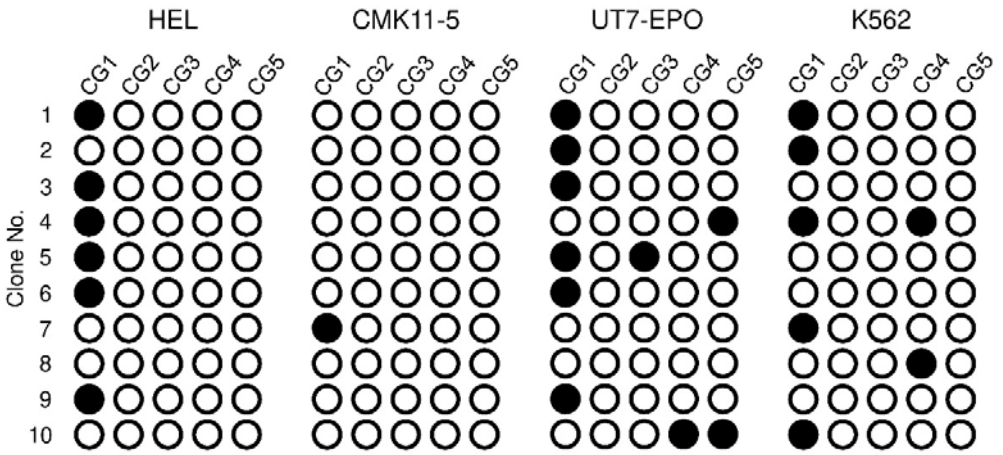

Supplementary Figure 8

DNA methylation status in the CA of *GFI1*-SE in erythro-megakaryocytic leukemia cell lines

CpG methylation status by bisulfite sequencing in the CA of *GFI1*-SE. Transverse rows and vertical lines represent each single clone and each CpG site, respectively. Solid and open circles indicate methylated and unmethylated CG sites, respectively. Five CpG sites in the CA of *GFI1*-SE are indicated in Supplementary Figure 7.

Supplementary Figure 9

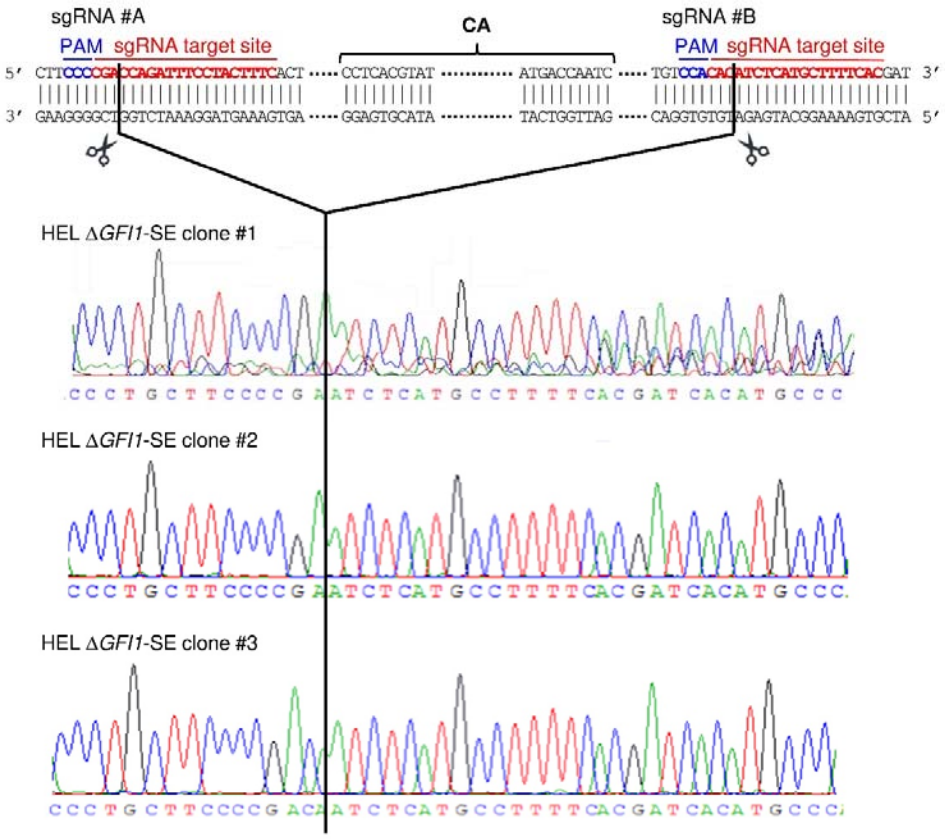

Supplementary Figure 9

Generation of Δ*GFI1*-SE HEL cells by CRISPR-Cas9

Establishment of Δ*GFI1*-SE sublines of HEL cells. The upper part shows a schematic diagram of the establishment of subclones harboring a *GFI1*-SE knockout allele using the CRISPR-Cas9 genome editing system. The vertical lines indicate the predicted Cas9 cleavage between two sgRNA sequences. The lower part shows Sanger-sequencing results

of the targeted region of three Δ*GFI1*-SE sublines (Δ*GFI1*-SE).

Supplementary Figure 10

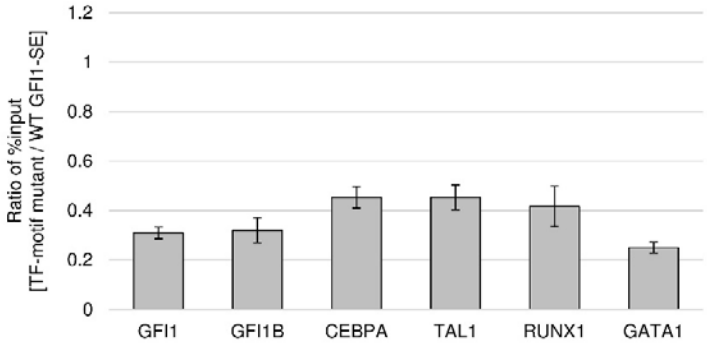

Supplementary Figure 10

Reduction of direct TF recruitment in single TF-motif mutated *GFI1*-SE in Δ*GFI1*-SE cells

ChIP-qPCR analysis for GFI1, GFI1B, CEBPA, TAL1, RUNX1, and GATA1 after reinduction of each single TF-motif mutant vector or wild-type *GFI1*-SE vector into Δ*GFI1*-SE cells. Data are shown as the ratio of % input of indicated TFs on each TF-motif mutated *GFI1*-SE to that in wild-type *GFI1*-SE. Experiments were performed independently three times and the means (± SD) are shown.

Supplementary Figure 11

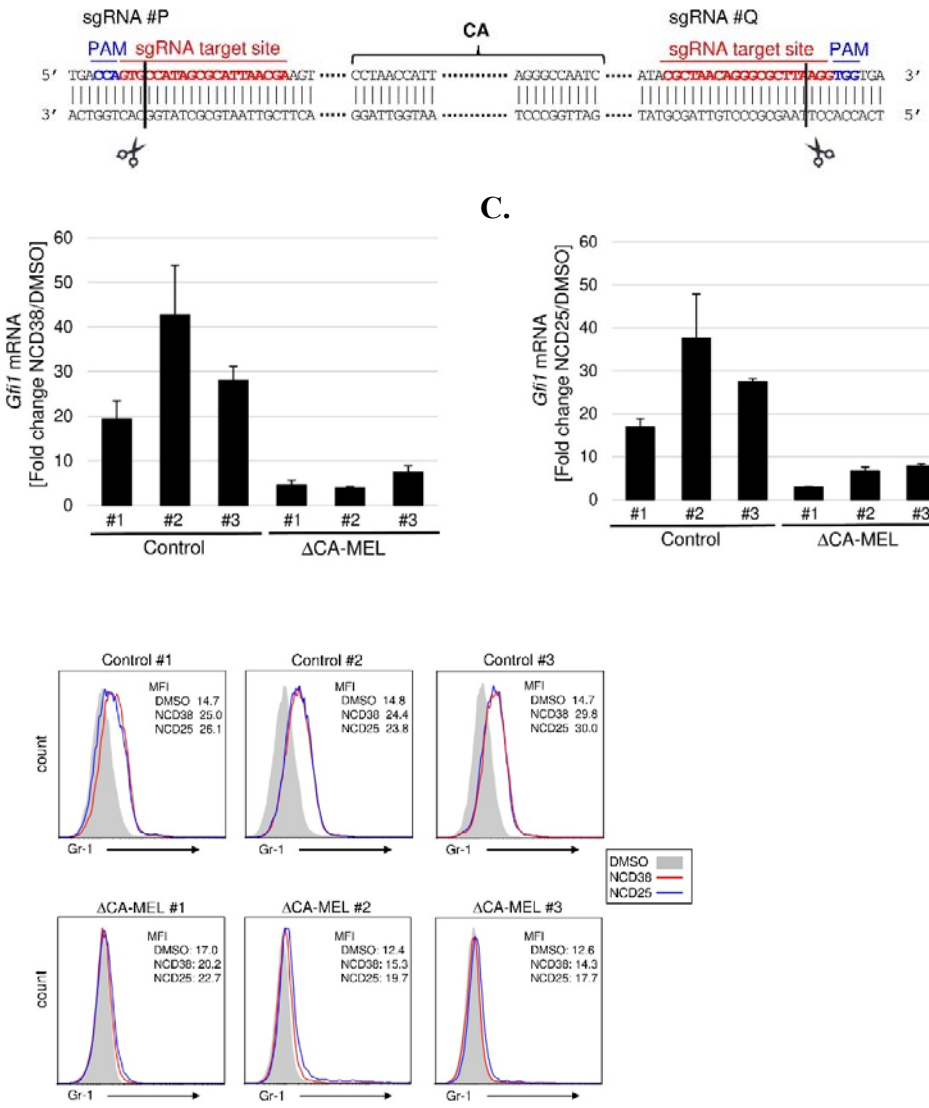

Supplementary Figure 11

Attenuation of myeloid differentiation by NCD38 and NCD25 in ΔCA murine erythroleukemia (MEL) cells

(a) Schematic diagram of the establishment of subclones harboring the ΔCA allele (MEL-

ΔCA) using the CRISPR-Cas9 genome editing system. The vertical lines indicate the predicted Cas9 cleavage between two sgRNA sequences. (b, c) Fold change of *Gfi1* mRNA after 48-hour treatment with 2 μM NCD38 and NCD25. The fold change was calculated in each subline by dividing *Gfi1* mRNA level in NCD38 or NCD25 by that in DMSO. Experiments were performed independently three times and the means (± SD) are shown. (d) FACS analysis of Gr-1 (Ly-6G). Histogram shows Gr-1 expression on the cell surface of each subline after 48-hour treatment with 2 μM NCD38, NCD25 or DMSO. The filled histograms indicate DMSO-treated cells. The mean fluorescence intensity (MFI) is shown. The experiments were performed independently twice and representative data are shown.

Supplementary Figure 12

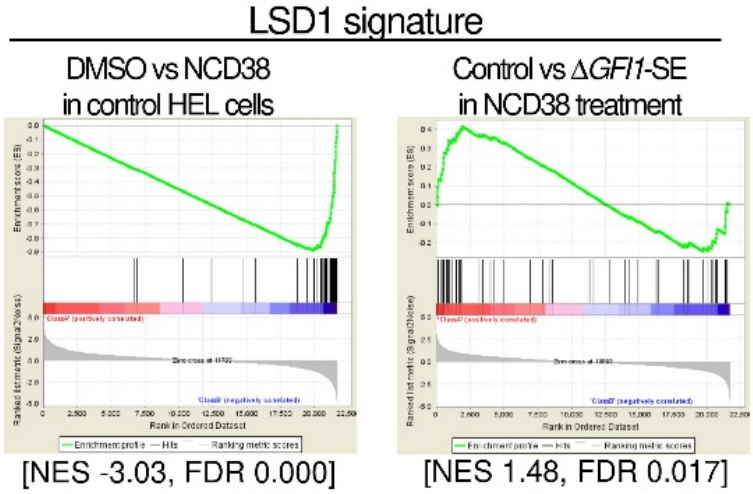

Supplementary Figure 12

GSEA analysis of the LSD1 signature

The left and right panels present results from comparison between DMSO treatment and NCD38 treatment in control HEL cells and between control HEL cells and Δ*GFI1*-SE HEL cells upon NCD38 treatment, respectively. The normalized enrichment score (NES) and the false discovery rate (FDR) q-value in GSEA are presented at the bottom of each panel. A gene set for the LSD1 signature is listed in Supplementary Table 2.

Supplementary Figure 13

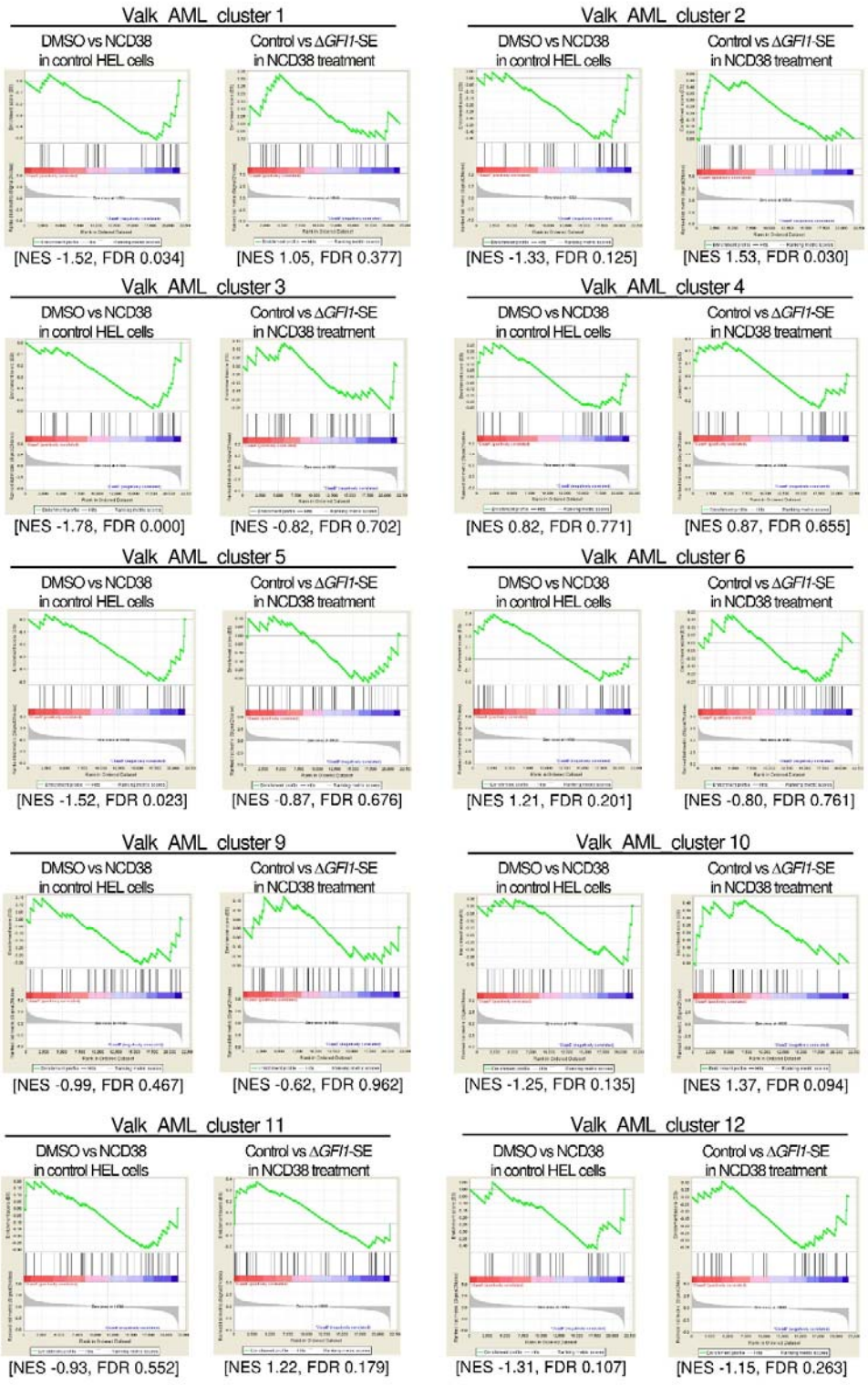

Supplementary Figure 13, continued

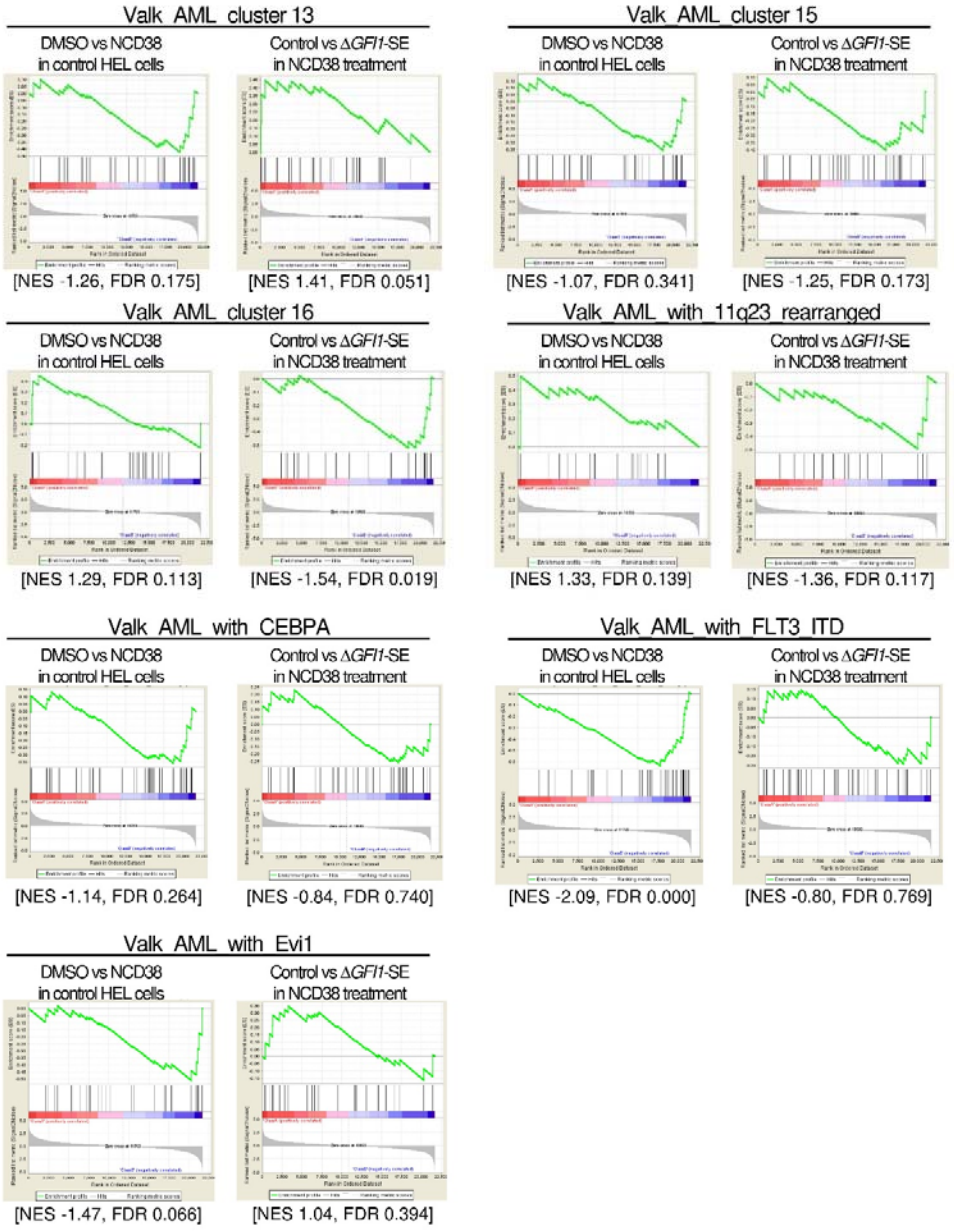

Supplementary Figure 13

GSEA analysis of gene sets of AML from datasets previously reported by Valk et al.

In each AML cluster signature, the left and right panels present results from the comparison between DMSO treatment and NCD38 treatment in control HEL cells and between control HEL cells and Δ*GFI1*-SE HEL cells upon NCD38 treatment, respectively. The normalized enrichment score (NES) and the false discovery rate (FDR) q-value in GSEA are presented at the bottom of each panel. Gene sets for each AML cluster signature are listed in Supplementary Table 2.

Supplementary Table 1. Primers and sgRNAs

Primers for RT-PCR

human *GFI1*	Forward	CTCGGAGTTTGAGGACTTCTG
	Reverse	CCGCTCCATGAGTACGGTTTG
human *GAPDH*	Forward	GAAGGTGAAGGTCGGAGTC
	Reverse	GAAGATGGTGATGGGATTTC
murine *Gfi1*	Forward	CTATCCCTGTCAGTACTGTGGC
	Reverse	CTTGAAGCCTGTGTGCTTTCTG
murine *Gapdh*	Forward	AGGTCGGTGTGTGAACGGATTTG
	Reverse	TGTAGACCATGTAGTTGAGGTCA

Primers for ChIP-qPCR

human *GFI1*-SE	Forward	TGTCATTTTCTTCATTTTGGGGG
	Reverse	CCCAGAGCAACTCCTAAGTG
murine CA	Forward	CCAGCCTAACTGTCAGAGGTAAA
	Reverse	TCCGCTCCCCTATTTTCTAAGAG

Primers for bisulfite-specific PCR

First half part of CA	Forward	TAAAGGTGATTTTTGTTTGTTTGAG
	Reverse	ATTCTTACCAACTATTAAATTCAACCTATA
Second half part of CA	Forward	TTTATATAATATAAGTTGAGTTTTTTTT
	Reverse	AATTAATTTCCTTCAACAACCTAAC

sgRNAs for enhancer deletion

human *GFI1*-SE	sgRNA #A	GAAAGTAGGAAATCTGGTCGGGG
	sgRNA #B	GTGAAAAGGCATGAGATGTGTGG
murine CA	sgRNA #P	TCGTTAATGCGCTATGGCACTGG
	sgRNA #Q	CGCTAACAGGGCGCTTAAGGTGG

Genotyping primers for detecting enhancer deletion

human *GFI1*-SE	Forward	CCTGATTCTGTGCCTTCTTCATAC
	Reverse	GAGTGTGGTTTGACTGTGGTATC

murine CA	Forward	GAAAAATCTGGCATGTCTGTCCC
	Reverse	CGGTTTGATTGTTGACACCTGTT

Primers for generating vectors for luciferase assays

cloning *GFI1*-SE	Forward	TTAGAGGAGGCACTGAAAGCAAG
	Reverse	CATACTTGTAAGCCCAGCTACTTG
deletion of non-CA	Forward	CTTACCTTGCTTTCAGTGCCTCC
	Reverse	ACACCCTCACGTATCTAATAGGAC
deletion of CA	Forward	AGTCCTATTAGATACGTGAGGGTG
	Reverse	GTTGTTGTTGAGATGGAGTCTTGC
GFI1/GF1B motif mutant #1	Forward	ACTCTAATCCTA**C**TCATTGCCTTCTTTC
	Reverse	CTAGAAAACCGTTAAGAAGGAGGAAGTT
GFI1/GF1B motif mutant #2	Forward	AGTGGGAGTAA**C**TCTCCAAACCACTCTC
	Reverse	AAGTTGATAAACTTCCTCCTTCTTAACG
RUNX1 motif mutant	Forward	CTAAGGCCACAGCTGCTAAGGACAAAAG
	Reverse	CTAAGG**GG**ACAGCTGCTAAGGACAAAAG
GATA1 motif mutant	Forward	ACTTTATCTAGGTTTGCAATCAGGAAGC
	Reverse	ACTTTA**C**CTAGGTTTGCAATCAGGAAGC
CEBPA motif mutant #1	Forward	CTTTATCTAGGTTTGC**CC**TCAGGAAGCTGT
	Reverse	TCTAAGGCCACAGCTGCTAAGGACAAAAGC
CEBPA motif mutant #2	Forward	AACACTCGTGGAGAA**GG**TGGAAAGAAGGCA
	Reverse	GCTCAGGAAGCACAAGTAGCTGTAAACCAC
TAL1 motif mutant	Forward	AGGTTGAATCCAA**G**AGTT**T**GTAAGAACCAG
	Reverse	GTAGCAAACTGGACAGAGCACAGCCTGTCC

* The mutation in each motif site is underlined.

Supplementary Table 2. Gene sets for GSEA analysis

A. REGULATION_OF_GRANULOCYTE_DIFFERENTIATION

ADIPOQ	C1QC	CUL4A	HAX1	HCLS1	IL5	INPP5D
LEF1	MLL5	OGT	PRDM16	RARA	RUNX1	TESC
TRIB1	ZBTB46					

B. KAMIKUBO_MYELOID_CEBPA_NETWORK

ALDH2	ANXA1	CAMP	CASD1	CD177	CEBPA	CSF2RA
CYBB	DGAT2	EMR1	GLRX	HDC	HP	IL18
IRF8	ITGAM	LBP	LCN2	LGALS1	LTF	MMP8
PGD	PRTN3	RAB31	S100A8	S100A9	SERPINB1	SPINT2

C. Differentially expressed genes found during erythroid development

ALAS2	ANK1	ARPC1B	ATP5G1	BDNFOS	BTG1	C11orf17
C19orf48	C19orf6	C1QBP	CA1	CAPG	CCDC114	CCL18
CCL2	CCL5	CCT6A	CD44	CECR1	CSTB	CTSH
CYBA	CYBASC3	CYP27A1	EGR1	ERAF	EYA3	FADS2
FCGRT	FCN1	FKBP5	GDF15	GIPC1	GYPC	H3F3A
HBA1	HBB	HBG1	HBM	HLA-DQA1	HLA-DRA	HMGN1
IGHG1	IL8	ILF3	ITLN1	KCNH2	KHSRP	KIAA1727
LIPA	LOC388588	LOC399761	LOC730200	LXN	LYZ	MGC4677
MMP9	NDUFA3	NOP5/NOP58	NUDT4	PLA2G7	PRG1	PRSS1
PSAP	PSMA2	REXO2	RHAG	RNASE1	RPL22L1	SELENBP1
SLC12A9	SLC25A37	SNHG5	SOD2	STK11	TINP1	TPSAB1
TRIB3	TSPAN17	TYMS	UBE2D3	UQCRQ	VAV2	WDR36

D. WELCH_GATA1_TARGETS

ABCB10	ALAD	ALAS2	ANK1	BACH1	EPB49	FTL

GSTT2	HBZ	HEBP1	HMBS	KLF1	MAFG	MAFK
NFE2	PPOX	SLC4A1	STOM	TFRC	UROD	UROS
ZFPM1						

E. Valk_AML_cluster_7

ANK1	C5ORF4	CLCN3	DNAJC6	EPB41	GAPVD1	GDF15
GYPE	HBBP1	HBZ	KCNH2	KEL	MYL4	OSBP2
PDZK1IP1	RAP1GAP	RHAG	RHD	SELENBP1	SLC25A37	SLC2A1
SLC6A8	SLC6A9	SPTB	TAL1	TNS1	TPM1	TRIM10

F. Valk_AML_cluster_8

ABCG2	ANK1	ARHGEF12	BCAM	C5ORF4	CDC42BPA	CDH1
DCAF11	FECH	GYPA	GYPB	MOSPD1	MXI1	OPTN
OSBP2	PBX1	RHCE	RHD	SELENBP1	SLC6A8	SNCA
TAL1	TMEM158	TNS1	TRAK2	TSPAN5		

G. LSD1 signature

ACVRL1	ARHGEF11	BST2	CALHM2	CCR2	CCSER2	CLEC4A
CNR2	CORO2A	CTSV	EFNA4	ERG	FCGR1B	FCGR2B
FCRLA	FOSL2	GCNT1	GFI1	GFI1B	HLA-DMB	HVCN1
HYLS1	IL18R1	IL18RAP	IL4I1	ISY1-RAB43	KIAA0513	LAIR1
LMO4	LOC388242	LPXN	METTL7A	MILR1	OIT3	OSBPL11
P2RY14	PI16	PIK3C2B	PLD2	PNRC1	PPP1R13B	PROCR
PRR9	RAB43	RASSF4	S1PR1	SELL	SIDT2	SIGLEC17P
SLC35F6	SLC7A8	SNX21	SPTAN1	STAB1	TIGD3	TLR1
TMEM243	TNFRSF10D	TNFSF10	TPM4	TRAF5	ZBTB46	

H. Valk_AML_cluster_1

ATF3	ATP10A	BHLHE41	BLNK	BMI1	COBLL1	DPP4

FHL1	GPR126	IGHM	IRF7	JUN	KCNA5	KIF17
LTBP3	MECOM	MEF2C	MMRN1	NR4A2	PCDH9	PROM1
PRR16	SLC2A3	SLC38A1	SOCS2	SPAG6	SPIB	TRPS1

I. Valk_AML_cluster_2

ARHGAP22	CCL1	CLU	DOCK1	EZR	GLI2	GOLGA8A
GOLGA8B	GPR56	GRB10	GUCY1A3	HBB	HOXA5	HOXB2
IL2RA	JAG1	KCNK5	LAPTM4B	LPIN1	MAP4K4	PDE3B
PIM1	PLA2G4A	PLS1	PTP4A3	SCHIP1	SRSF8	TRIM16
TRPC2						

J. Valk_AML_cluster_3

ADCY2	AGTPBP1	AIM1	ARHGAP22	BLVRA	CCL1	CEBPD
COL4A5	DOCK1	ENPP4	FAM30A	FCGRT	GAS2	GPR56
IL17RA	IL6ST	LAPTM4B	MAP7	NET1	PBXIP1	PDGFD
PIEZO2	PLS1	QPRT	RAP2A	SCN9A	SEPP1	SERPINB8
SH2D1A	SMC4	TNFRSF4	TRIM16	WBP5		

K. Valk_AML_cluster_4

ABCB1	B4GALT6	C18ORF1	CAPN2	CD7	CFD	CSDA
CTNNA1	CYFIP1	DRAM1	FZD6	HPGDS	HPS4	IGFBP7
IKZF2	IL4R	ITGA4	KLF2	LRP10	NDFIP1	P2RX5
PMS2L2	PMS2P3	PRR5L	RAB13	TRAT1	TRDV2	TRIB1
TSPAN7	TUBB6	UGT2B28				

L. Valk_AML_cluster_5

CAMK1	CCR1	CD86	EFHD2	EPB41L3	FAM198B	GNS
HNMT	IFNGR2	KCNQ1	LILRA1	LILRA6	LILRB1	LILRB2
LILRB3	MAFB	NOD2	PILRA	PSAP	PTAFR	RASSF4

SIGLEC7	SIRPA	SIRPB1	SLC15A3	SMPDL3A	STS	TFEB
TLR8	TYMP	UBE2D1	VCAN	VDR		

M. Valk_AML_cluster_6

ADCY2	BST2	CAT	CD74	CEP70	CORO1A	DPPA4
DPYSL3	DSC2	FAM110B	FAM174B	FOXC1	FOXF2	FTO
GPC4	HIGD1A	HLA-DPA1	HLA-DRA	HOXB3	KIAA0930	LTBP1
NT5DC3	PECAM1	PIEZO2	PLXNB1	RGS10	RSL1D1	SLC27A6
SMC4	SNCAIP	TTC27	TUBGCP4	XPA		

N. Valk_AML_cluster_9

AK5	BAHCC1	CBFB	CD1C	CD59	CD81	CHI3L1
CHST12	CLEC10A	CLIP2	CLIP3	COLEC12	DHRS3	EMID1
FAM105A	FAM171A1	FCGR2B	ICAM4	MGLL	MN1	MSLN
MTMR11	MYH11	NDE1	NRP1	NT5E	PAPSS2	PTPRM
RPS6KA2	RUNX3	SPARC	ST18	TGFBI	TPPP3	VSIG4

O. Valk_AML_cluster_10

ARHGEF17	AZU1	BAALC	BCL7A	C3AR1	CD22	CFD
CHRDL1	CRIM1	EEF1A2	F2RL1	FAM30A	FLNB	GNAI1
IGHM	LPHN1	MLLT3	MN1	NPDC1	PAWR	PIK3C2B
PPP1R16B	PRKD2	RBPMS	RNASE2	SETBP1	SMAGP	SNED1
SORBS3	SPON1	SPRY1	SPTBN1	TPM2		

P. Valk_AML_cluster_11

ALDH2	APP	ASS1	CD200	CD34	CIITA	CISH
CLIC4	DAB2	DAPK1	DNM1	DPYSL2	DUSP7	EGFL7
EVL	FYN	GAS2L1	GIMAP5	GIMAP6	H1F0	IFITM1
ITGA6	KCNN4	KLF9	KYNU	LHFPL2	LPAR6	MDFIC

MYO5C	PALM	REEP5	SERPINB9	SLC38A1	SPARC	ST3GAL5
VEGFA						

Q. Valk_AML_cluster_12

AFF2	ALADL1	ARHGAP4	AZI2	CALR	CST7	FGF13
GABRE	GALNT3	HGF	LAMC1	LGALS9	MEG3	MFNG
MST1	MXRA7	NKX3-2	NRIP1	P4HB	PCBP3	PRODH
PTCH1	PTGDS	PTGER1	RAB5B	SIX3	SKAP2	STXBP1
TMEM87A	VCL					

R. Valk_AML_cluster_13

ADCY7	ADRA2C	BAIAP3	C11ORF21	C11ORF9	C15ORF39	CACNA2D2
CAV1	FBLN5	GRK5	HSPG2	IL5RA	ITGB4	KDM4B
LAT2	LCP1	NBL1	NCALD	PNMT	POU4F1	PSD3
RFL	ROBO1	RUNX1T1	SLC25A1	STK32B	THSD7A	TRH
VLDLR	VOPP1					

S. Valk_AML_cluster_15

ARHGEF3	ATN1	BASP1	CD52	CEACAM8	CTNNA1	DRAM1
ECHDC2	EPB41L2	FADS1	GNA12	GRAMD1B	HOXA10	HOXA9
HOXB2	HOXB5	HSPB1	IGF2BP2	IGHM	KLF9	MEIS1
NDFIP1	RUNX1	SEL1L3	SFXN3	SH3TC1	SLC16A1	SUCLG2
TBL1X	TNS3	TUBB6				

T. Valk_AML_cluster_16

ADCY9	AK2	AKR7A2	APOC2	BRE	C1ORF54	C20ORF103
C3ORF14	CACNA2D3	CADM1	CD70	CLSTN2	DACH1	GGA2
ITGA7	KCNE1L	KCNN2	MBNL1	PENK	RET	RPP25
TDRD7	TGM5	TKTL1	TRPM4	UVRAG		

U. Valk_AML_with_11q23_rearranged

APOC2	C1ORF54	C20ORF103	C3ORF14	CACNA2D3	CADM1	CD70
CES1	DACH1	HIF1A	ITGA7	KCNE1L	LOC283683	MSLN
NXT2	P2RY2	PENK	RET	TGM5	TKTL1	TRPM4
UVRAG						

V. Valk_AML_with_CEBPA

ARHGEF3	ATN1	B4GALT6	BASP1	CAMP	CD38	CD7
CEACAM8	CEBPA	CTNNA1	DLC1	GALC	GNA12	HOXA9
HOXB2	HPGDS	HSPB1	IGF2BP2	IGHM	IGLL1	ITM2A
LCN2	LTF	MEST	MMP8	NDFIP1	PGLYRP1	PRR5L
SEL1L3	SFXN3	SLC16A1	SUCLG2	TBL1X	TNS3	TRDV2
TRIB1	TUBB6					

W. Valk_AML_with_FLT3_ITD

ADCY2	APP	BAHCC1	COL4A5	CYSLTR2	ENPP2	GOLGA8A
GOLGA8B	GPR56	HOXA4	HOXA5	HOXA9	HOXB2	HOXB3
HOXB5	HOXB6	IL1RAP	IL2RA	KCNK5	LAPTM4B	LCT
LGALS3BP	LYRM1	MAGED1	MAP1A	MMP2	MRC1	NR6A1
PBX3	PDE4B	PDGFD	PIEZO2	PIM1	QPRT	SEPP1
SMC4	SOCS2	TARP	TRIM16	TRPC2		

X. Valk_AML_with_EVI1

AZU1	CD34	CFD	CRIM1	DMXL2	EEF1A2	F2RL1
FAM30A	GNAI1	IGHM	LPHN1	MN1	NPDC1	PAWR
PIK3C2B	PPP1R16B	PXDN	RBPMS	RNASE2	RNASE3	SEPX1
SMAGP	SORBS3	SPRY1	SPTBN1			

Supplementary Table 3. List of genes influenced by *GFI1*-SE depletion

Genes that were induced more than two-fold by NCD 38 but whose inductions were attenuated by less than 50% via *GFI1*-SE depletion

Gene Symbol	Fold Change [DMSO vs NCD38 in control HEL cells]	Fold Change [Control vs ΔGFI1-SE in NCD38 treatment]	Fold Change [DMSO vs NCD38 in CMK11-5 cells (Dataset: GSE68348)][4]
LOC101928012	12.35	5.50	13.43
PRR9	10.62	4.44	7.00
GFI1	8.05	2.85	9.07
S1PR1	6.27	2.59	7.39
SLC45A3	6.24	3.08	3.17
TEK	5.33	2.28	3.24
TRGJP2	4.37	1.32	2.41
STYK1	3.56	1.56	2.73
ERG	3.54	1.76	4.58
CD200R1	2.69	1.22	7.98
RP11-702L15.4	2.36	1.18	NA
IGFBP4	2.08	0.96	2.47
RNU6-795P	2.07	0.83	NA
MIR296	2.06	0.71	NA
RP11-758M4.4	2.05	0.92	NA
RP11-661A12.4	2.02	0.91	NA
RPL23AP32	2.00	0.93	1.99

Genes that were attenuated by less than 50% by NCD 38 but whose reductions were recovered more than two-fold via *GFI1*-SE depletion

Gene Symbol	Fold Change [DMSO vs NCD38 in control HEL cells]	Fold Change [Control vs ΔGFI1-SE in NCD38 treatment]	Fold Change [DMSO vs NCD38 in CMK11-5 cells (Dataset: GSE68348)][4]
THBS1	0.41	1.07	0.33
CCR4	0.41	0.94	0.91

RHD	0.42	0.84	0.15
FAM19A3	0.46	0.93	0.45
RNA5SP302	0.49	1.03	NA

NA; not available in this data set (GSE68348) due to differences between the platforms used for separate analyses (Affymetrix vs. Agilent).

Supplementary References

1. Tohyama K, Tohyama Y, Nakayama T, Ueda T, Nakamura T, Yoshida Y. A novel factor-dependent human myelodysplastic cell line, MDS92, contains haemopoietic cells of several lineages. *British journal of haematology* 1995 Dec; **91**(4)**:** 795-799.

2. Shimazu Y, Hishizawa M, Hamaguchi M, Nagai Y, Sugino N, Fujii S, *et al.* Hypomethylation of the Treg-Specific Demethylated Region in FOXP3 Is a Hallmark of the Regulatory T-cell Subtype in Adult T-cell Leukemia. *Cancer Immunol Res* 2016 Feb; **4**(2)**:** 136-145.

3. Yamamoto R, Kawahara M, Ito S, Satoh J, Tatsumi G, Hishizawa M, *et al.* Selective dissociation between LSD1 and GFI1B by a LSD1 inhibitor NCD38 induces the activation of ERG super-enhancer in erythroleukemia cells. *Oncotarget* 2018 Apr 20; **9**(30)**:** 21007-21021.

4. Sugino N, Kawahara M, Tatsumi G, Kanai A, Matsui H, Yamamoto R, *et al.* A novel LSD1 inhibitor NCD38 ameliorates MDS-related leukemia with complex karyotype by attenuating leukemia programs via activating super-enhancers. *Leukemia* 2017 Nov; **31**(11)**:** 2303-2314.